Single-Molecule Magnets

DOI: 10.1002/ange.201008180

Wheel-Shaped $Er^{III}Zn^{II}_3$ Single-Molecule Magnet: A Macrocyclic Approach to Designing Magnetic Anisotropy**

Aika Yamashita, Akiko Watanabe, Shigehisa Akine, Tatsuya Nabeshima, Motohiro Nakano, Tomoo Yamamura, and Takashi Kajiwara**

Single-molecule magnets (SMMs)[1–6] are chemically and physically interesting compounds that exhibit hitherto unobserved magnetic properties. To prevent reversal of the molecular magnetic moment, the use of heavy lanthanide ions is becoming popular because of their large spin multiplicity and large magnetic anisotropies in the ground state.[3–6] Lanthanide ions exhibit flexibility in magnetic anisotropy, which is another advantage of Ln^{III}-based SMMs that is attributable to the flexible design and control of the ligand-field (LF) anisotropy. These anisotropies are correlated through Stevens' factor θ_m as $B^n_m = A^n_m\langle r^m\rangle\theta_m$, where B^n_m denotes the mth-order magnetic anisotropy parameters (m is 2, 4, or 6 for lanthanide ions; n varies between 0 and m; second-order terms of B^0_2 and B^2_2 correspond to the axial and rhombic anisotropic parameters D and E), and $A^n_m\langle r^m\rangle$ denotes the LF anisotropy parameters.[7] Therefore, Ln^{III} complexes have a wide scope in the synthetic design of anisotropic magnets. Although many complexes including one or more heavy lanthanide ions are reported to be SMMs, most of them were synthesized in a fortuitous manner without design of the magnetic anisotropy. We have demonstrated previously that an axial LF, whereby donor atoms with higher negative charges are located along the principal axis, induces a strong Ising-type anisotropy of Tb^{III} and Dy^{III} ions.[5] This type of LF anisotropy is easily achieved in an accidental manner, and thus a wide variety of Tb^{III} and Dy^{III} SMMs have been reported. On the contrary, Er^{III}-based SMMs are rare.[6] When the second-order anisotropy terms are dominant, magnetic anisotropy of the Er^{III} ion has opposite features to those of Tb^{III} and Dy^{III} ions, since the θ_2 parameter of the Er^{III} ion is positive, whereas those of the Tb^{III} and Dy^{III} ions are negative. This is the reason why Er^{III}-based SMMs are rare: to achieve easy-axis anisotropy for Er^{III}, an LF from equatorial donors is predicted to be needed, which is achieved by using the opposite strategy to those for Tb^{III} and Dy^{III} ions. Hence investigation of the proper design of Er^{III} SMMs is needed to establish a common synthetic strategy for Ln^{III}-based SMMs. Herein we report an example of an Er^{III} SMM which was achieved by design of magnetic anisotropy for the first time.

We found that phenoxo oxygen donors have higher negative charges than other donor atoms.[5] To achieve an equatorial LF, we focused on the macrocyclic Schiff base and oxime ligands shown in Scheme 1, which provide a metal-

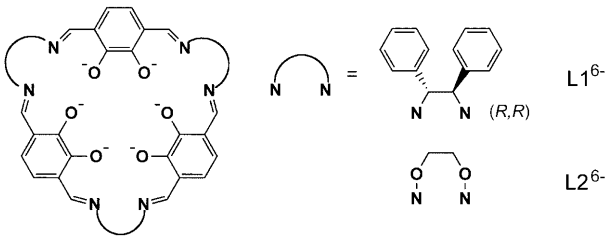

Scheme 1. Structures of macrocyclic ligands.

lacrown coordination environment[3j,8] for the central metal ion with six phenoxo oxygen donors and have a rigid and planar framework owing to the π-conjugated moieties. The ligands are formed by condensation of 2,3-dihydroxybenzene-1,4-dicarbaldehyde and a diamine in the presence of metal ions as templates. The six phenoxo oxygen atoms are in equatorial positions around a central Ln^{III} ion, and hence an equatorial LF is produced. We have reported syntheses and structures of mixed-metal tetranuclear complexes constructed with $L2^{6-}$,[9] of which the oxime ligand showed a slight deviation from an ideal plane because of the longer N–N distance of the diamine. Hence, we decided to employ an ethylenediamine derivative to achieve a more planar structure of the complex.

The wheel-shaped tetranuclear complex $[Er^{III}Zn^{II}_3(L1)(OAc)(NO_3)_2(H_2O)_{1.5}(MeOH)_{0.5}]$ (**1**) was synthesized by reaction of $Er(NO_3)_3\cdot 6H_2O$, 2,3-dihydroxybenzene-1,4-dicarbaldehyde, (*R*,*R*)-1,2-diphenylethylenediamine, and $Zn(OAc)_2\cdot 2H_2O$ in 1:3:3:3 ratio (see Experimental Section;

[*] A. Yamashita, A. Watanabe, Prof. Dr. T. Kajiwara
Faculty of Science, Nara Women's University
Nara, Nara 630-8506 (Japan)
Fax: (+81) 742-20-3402
E-mail: kajiwara@cc.nara-wu.ac.jp
Prof. Dr. S. Akine, Prof. Dr. T. Nabeshima
Graduate School of Pure and Applied Sciences, University of Tsukuba
Tsukuba, Ibaraki 305-8571 (Japan)
E-mail: nabesima@chem.tsukuba.ac.jp
Prof. Dr. M. Nakano
Graduate School of Engineering, Osaka University
Suita, Osaka 565-0871 (Japan)
Dr. T. Yamamura
Institute for Materials Research, Tohoku University
Aoba-ku, Sendai, Miyagi 980-8577 (Japan)

[**] This work was supported by The Sumitomo Foundation, as well as a Grant-in Aid for Scientific Research of Priority Areas (Panoscopic Assembling and High Ordered Functions for Rare Earth Materials) and Scientific Research (C) from the Ministry of Education, Culture, Science, Sports and Technology (Japan).

Supporting information for this article is available on the WWW under http://dx.doi.org/10.1002/anie.201008180.

Figure 1). In this complex, the macrocyclic Schiff base ligand $L1^{6-}$ offers hexadentate and tetradentate coordination sites for Er^{III} and Zn^{II}, respectively. An Er^{III} ion in **1** is nine-

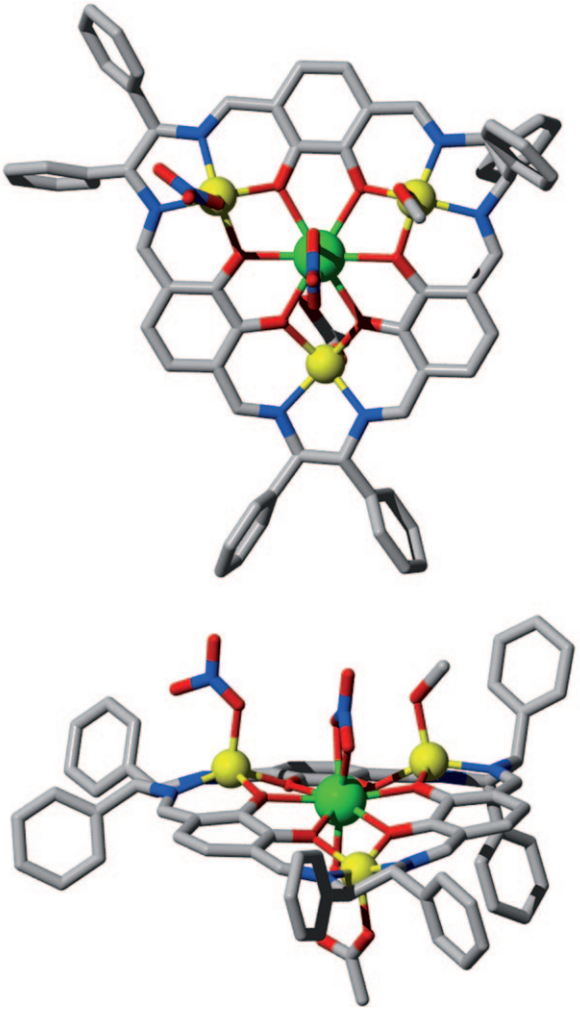

Figure 1. Top view (top) and side view (bottom) of the molecular structure of tetranuclear **1**. Green Er^{III}, yellow Zn^{II}, red O, blue N, light gray C.

coordinate with the six phenoxo oxygen atoms of $L1^{6-}$ at equatorial positions (O1–O6, Er–O 2.428(3)–2.468(3) Å, Figure S1 in the Supporting Information), and three oxygen atoms from water (O10, 2.273(3) Å) and a nitrate anion (O7 and O8, 2.416(4) and 2.415(3) Å) at axial positions. The equatorial plane of the six phenoxo oxygen atoms is slightly bent; two oxygen atoms (O1 and O4) are located 0.456(2) and 0.338(2) Å above the ideal plane, and the other four oxygen atoms 0.095(2)–0.307(2) Å below the plane. However, the deviations are relatively small compared to the Er–O distances, and it can be concluded that the six phenoxo oxygen donors form a strong equatorial LF, which is dominant for easy-axis magnetic anisotropy of the Er^{III} ion. The Zn^{II} ions are in square O_2N_2 coordination sites of $L1^{6-}$ and further ligated by supporting acetate, nitrate, or methanol ligands at axial positions to complete square-pyramidal coordination.

Density functional calculations were carried out for **1** to estimate the Mulliken charges of the donor oxygen atoms (Figure S1 in the Supporting Information). As expected, the phenoxo oxygen atoms had higher negative charges, and the formation of an equatorial LF around the Er^{III} ion was confirmed.

The SMM features of **1** were investigated by ac magnetic susceptibility measurements. When the ac susceptibility was measured under zero external field, no out-of-phase signal (χ'') was observed, which indicates the presence of fast relaxation via a quantum tunneling process. To prevent the tunneling relaxation, a weak external field of up to 1000 Oe was applied (Figure S2 in the Supporting Information). Compound **1** exhibited slow magnetic relaxation under an external field of 1000 Oe (Figure 2); χ'' exhibits its frequency

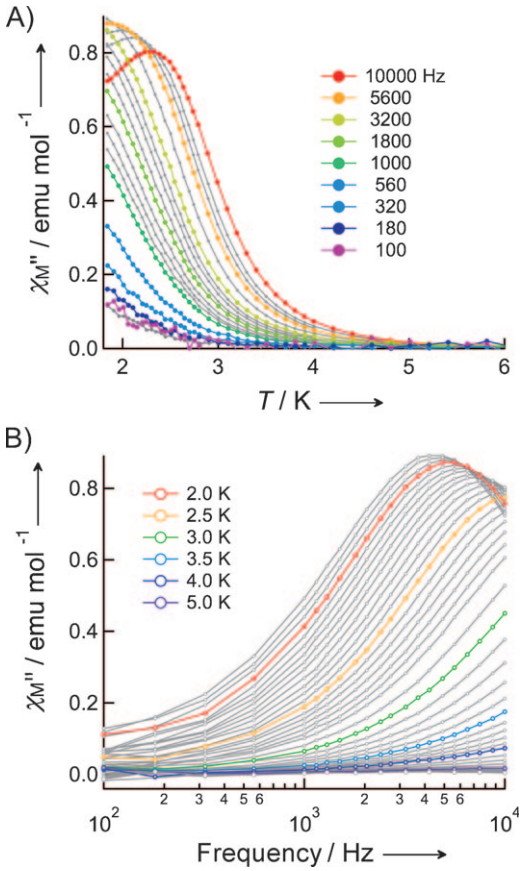

Figure 2. A) Temperature and B) frequency dependence of χ_M'' values of **1** measured under 1000 Oe external field. The solid curves are guides for the eye.

dependence by the peaks observed in the range of 1.85–2.5 K. Cole–Cole and extended Debye analyses (Figures S3 and S4 in the Supporting Information) revealed that the thermal relaxation occurs by single processes with α parameters varying in a narrow range of 0.07–0.15 (at 1.85–3.0 K), which is a characteristic of SMMs.

Using the obtained relaxation time τ, an Arrhenius analysis was carried out (Figure 3). The energy barrier Δ/k_B and relaxation time τ_0 were estimated to be 8.1(4) K and

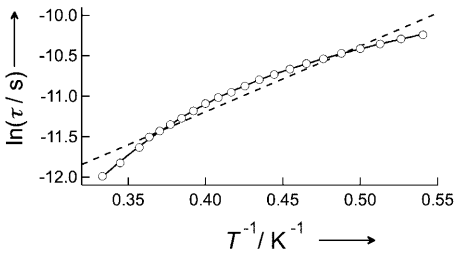

Figure 3. Arrhenius plot for **1** under 1000 Oe external field. The solid curves and dashed lines correspond to the Arrhenius laws with kinetic parameters described in the main text.

$5.3(9)\times10^{-7}$ s, respectively, by linear analysis. However, the plot shows a slight bend at around $T^{-1}=0.42\ K^{-1}$, which suggests the presence of dual relaxation pathways.[10] Of the two pathways, one has a longer relaxation time $\tau_0^{(1)}$ with a lower energy barrier $\Delta^{(1)}/k_B$, whereas the other has a shorter relaxation time $\tau_0^{(2)}$ with a higher energy barrier $\Delta^{(2)}/k_B$. According to Christou's formula,[10] these low and high energy barriers were estimated as 3.7(3) and 24.6(9) K, respectively.

To reveal the fine structure of ground multiplets, the field dependence of the magnetization was measured for a randomly oriented microcrystalline sample in the temperature range of 2.0–60 K (Figure S5 in the Supporting Information). At 2.0 K, the magnetization rapidly increased to approximately 1 T, after which it gradually and linearly increased to 9 T. Because the sample was fixed with eicosane, the observations were considered to be the sum of distributions of the magnetization measured on applying the field from different directions to the principal axis. If the complex had an easy-axis anisotropy, magnetization showed a rapid saturation at approximately 1 T under the effect of the field along the principal axis, whereas it showed small and gradual increases under the effect of a field perpendicular to the principal axis. Hence, the observed features are typical of easy-axis anisotropy. The M versus HT^{-1} curve shows discriminating dependence on temperature. From this curve, it can be observed that the fast saturation in regions of low HT^{-1} occurs more rapidly when the temperature is increased. This suggests the presence of excited sublevels with a higher $|J_z|$ value than the ground sublevels. These results are well explained by assuming that the sublevels $|J_z\rangle=|\pm13/2\rangle$ or $|\pm11/2\rangle$ are the ground states, whereas $|\pm15/2\rangle$ are the nearest excited states.

In summary, we have reported the second example of an Er^{III}-based SMM, which was synthesized by design of magnetic anisotropy for the first time. Design and control of magnetic anisotropy for the Ln^{III} ion are possible by appropriately designing the LF anisotropy, not only for Tb^{III} and Dy^{III}, but also for Er^{III}. For Er^{III}, such an easy-axis anisotropy was achieved by employing a planar macrocyclic ligand. The idea presented here is common to Ln^{III} ions, and hence SMMs including Ho^{III} or Tm^{III}, which are currently unknown, should become realizable in the future. The observed barrier of **1** for moment flipping is rather low, and hence detailed analyses, including the quantification of the magnetic anisotropy parameters, is needed for a fine-tuning of LF anisotropy for better SMM features. Such an investigation is now in progress.

Experimental Section

Synthesis of **1**: A solution of $Zn(OAc)_2{\cdot}2H_2O$ (0.045 mmol) in methanol (8.7 mL) and a 0.05 M methanolic solution of $Er(NO_3)_3{\cdot}6H_2O$ (0.3 mL, 0.015 mmol) were added to a solution of 2,3-dihydroxybenzene-1,4-dicarbaldehyde (0.045 mmol) in chloroform. The solution was evaporated in vacuo, and the residue was dissolved in chloroform/methanol (0.5/1.0 mL). A 0.1 M methanolic solution of (*R*,*R*)-1,2-diphenylethylenediamine was added to the resulting solution. Orange crystals formed after slow evaporation of the solvent and were filtered off and dried in vacuo (24% yield). Elemental analysis [%] calcd for $\mathbf{1}{\cdot}H_2O{\cdot}3MeOH$: C 49.79, H 4.09, N 6.50; found: C 49.82, H 3.94, N 6.39.

Crystal data for $\mathbf{1}{\cdot}H_2O{\cdot}5MeOH$: $C_{73.5}H_{78}ErN_8O_{22}Zn_3$, $M_r=1788.81$, orthorhombic, $P2_12_12_1$, $a=17.6987(8)$, $b=19.4477(11)$, $c=22.5836(12)$ Å, $V=7773.3(7)$ Å^3, $Z=4$, $T=153$ K, $F(000)=3622$, $\mu(Mo_{K\alpha})=2.061$ mm^{-1}. Using 962 parameters, $wR_2=0.1011$ (17777 unique reflections), $R_1=0.0361$ (17435 reflections with $I>2\sigma(I)$). CCDC 805688 contains the supplementary crystallographic data for this paper. These data can be obtained free of charge from The Cambridge Crystallographic Data Centre via www.ccdc.cam.ac.uk/data_request/cif.

Magnetic susceptibility measurements were performed with a Quantum Design magnetometer PPMS-9. A mixture of the powdered sample and eicosane was heated to 320 K to melt eicosane and then cooled to 300 K to fix the microcrystals.

Received: December 25, 2010
Published online: March 23, 2011

Keywords: lanthanides · ligand effects · macrocyclic ligands · magnetic properties · zinc

[1] a) D. Gatteschi, R. Sessoli, *Angew. Chem.* **2003**, *115*, 278; *Angew. Chem. Int. Ed.* **2003**, *42*, 268; b) W. Wernsdorfer, R. Sessoli, *Science* **1999**, *284*, 133; c) S. M. J. Aubin, Z. Sun, L. Pardi, J. Krzystek, K. Folting, L. C. Brunel, A. L. Rheingold, G. Christou, D. N. Hendrickson, *Inorg. Chem.* **1999**, *38*, 5329; d) L. Thomas, F. Lionti, R. Ballou, D. Gatteschi, R. Sessoli, B. Barbara, *Nature* **1996**, *383*, 145; e) E. K. Brechin, *Chem. Commun.* **2005**, 5141.

[2] W. Wernsdorfer, S. Badhuri, C. Boskovic, G. Christou, D. N. Hendrickson, *Phys. Rev. B* **2002**, *65*, 180403.

[3] a) S. Osa, T. Kido, N. Matsumoto, N. Re, A. Pochaba, J. Mronzinski, *J. Am. Chem. Soc.* **2004**, *126*, 420; b) C. M. Zaleski, E. C. Depperman, J. W. Kampf, M. L Kirk, V. Pecoraro, *Angew. Chem.* **2004**, *116*, 4002; *Angew. Chem. Int. Ed.* **2004**, *43*, 3912; c) A. Mishra, W. Wernsdorfer, K. A. Abboud, G. Christou, *J. Am. Chem. Soc.* **2004**, *126*, 15648; d) C. Aronica, G. Pilet, G. Chastanet, W. Wernsdorfer, J. F. Jacquot, D. Luneau, *Angew. Chem.* **2006**, *118*, 4775; *Angew. Chem. Int. Ed.* **2006**, *45*, 4659; e) F. Mori, T. Nyui, T. Ishida, T. Nogami, K.-Y. Choi, H. Nojiri, *J. Am. Chem. Soc.* **2006**, *128*, 1440; f) S. Ueki, T. Ishida, T. Nogami, K.-Y. Choi, H. Nojiri, *Chem. Phys. Lett.* **2007**, *440*, 263; g) G. Novitchi, W. Wernsdorfer, L. F. Chibotaru, J.-P. Costes, C. E. Anson, A. K. Powell, *Angew. Chem.* **2009**, *121*, 1642; *Angew. Chem. Int. Ed.* **2009**, *48*, 1614; h) T. C. Stamatatos, S. J. Teat, W. Wernsdorfer, G. Christou, *Angew. Chem.* **2009**, *121*, 529; *Angew. Chem. Int. Ed.* **2009**, *48*, 521; i) F. Pointillart, K. Bernot, R. Sessoli, D. Gatteschi, *Inorg. Chem.* **2010**, *49*, 4355; j) T. T. Boron III, J. W. Kampf, V. L. Pecoraro, *Inorg. Chem.* **2010**, *49*, 9104.

[4] a) N. Ishikawa, M. Sugita, T. Ishikawa, S. Koshihara, Y. Kaizu, *J. Am. Chem. Soc.* **2003**, *125*, 8694; b) F. Branzoli, P. Carretta, M. Filibian, G. Zoppellaro, M. J. Graf, J. R. Galan-Mascaros, O. Fuhr, S. Brink, M. Ruben, *J. Am. Chem. Soc.* **2009**, *131*, 4387; c) K. Katoh, Y. Yoshida, M. Yamashita, H. Miyasaka, B. K. Breedlove, T. Kajiwara, S. Takaishi, N. Ishikawa, H. Isshiki, Y. F. Zhang, T. Komeda, M. Yamagishi, J. Takeya, *J. Am. Chem. Soc.* **2009**, *131*, 9967.

[5] T. Kajiwara, M. Nakano, K. Takahashi, S. Takaishi, M. Yamashita, *Chem. Eur. J.* **2011**, *17*, 196 – 205.

[6] a) M. A. AlDamen, J. M. Clemente-Juan, E. Coronado, C. Martí-Gastaldo, A. Gaita-Ariño, *J. Am. Chem. Soc.* **2008**, *130*, 8874; b) M. A. AlDamen, S. Cardona-Serra, J. M. Clemente-Juan, E. Coronado, A. Gaita-Ariño, C. Martí-Gastaldo, F. Luis, O. Montero, *Inorg. Chem.* **2009**, *48*, 3467.

[7] a) D. Schmitt, *J. Phys.* **1986**, *47*, 677; b) J. Sievers, *Z. Phys. B* **1982**, *45*, 289.

[8] a) C. M. Zaleski, J. W. Kampf, T. Mallah, M. L. Kirk, V. L. Pecoraro, *Inorg. Chem.* **2007**, *46*, 1954; b) C. M. Zaleski, E. C. Depperman, J. W. Kampf, M. L. Kirk, V. L. Pecoraro, *Inorg. Chem.* **2006**, *45*, 10022; c) A. J. Stemmler, J. W. Kampf, M. L. Kirk, B. H. Atasi, V. L. Pecoraro, *Inorg. Chem.* **1999**, *38*, 2807.

[9] S. Akine, S. Sunaga, T. Taniguchi, H. Miyazaki, T. Nabeshima, *Inorg. Chem.* **2007**, *46*, 2959.

[10] C. Lampropoulos, S. Hill, G. Christou, *ChemPhysChem* **2009**, *10*, 2397.

